Origin of Periodic, Chaotic, and Bistable Emission from Raman Lasers

R. G. Harrison and Weiping Lu[a]
Department of Physics, Heriot-Watt University, Edinburgh EH14 4AS, Scotland

P. K. Gupta
Laser Section, Bhabha Atomic Research Centre, Bombay, India
(Received 1 May 1989)

Single-mode homogeneously broadened Raman laser emission is shown to be mathematically reducible to a simple description similar to that of the Haken-Lorenz model. However, the physically distinct lasing mechanism involving a two-photon interaction with an equivalent two-level system in a noninverted state allows for considerably relaxed operating conditions where periodic, chaotic, and bistable behavior are identified. Results are in good accord with earlier experiments.

PACS numbers: 42.50.Tj, 42.55.Em

Emission from Raman lasers has been shown to exhibit pulsating instabilities and chaos over a relatively broad range of operating conditions including those for optimum lasing.[1] However, the origin of such behavior remains unexplained. In this Letter we provide a clear physical and mathematical description of the nonlinear dynamical behavior exhibited in this class of laser under conditions of single-mode homogeneously broadened operation.[2] We establish a mathematical similarity between the equations describing this system and those for a detuned two-level laser.[3-5] The systems are, however, physically distinct Raman lasing involving a two-photon interaction with an equivalent two-level system in a noninverted state. The conditions for the onset of instabilities are, as a consequence, found to be far less restrictive for Raman lasers, arising at or close to the first lasing threshold in some cases and for moderately bad cavity conditions such that the decay rate of the cavity field is not significantly greater than those of the active medium. Instabilities are found to occur asymmetrically with respect to the gain center and in this region which is shown to be optimum for lasing the emission also exhibits bistability. Period-doubling routes to chaos have so far been identified.

Raman emission is conventionally described using the coupled-wave approach of nonlinear optics.[6] Alternatively this process may be regarded as a three-level atomic-molecular interaction[7] with a pump field (amplitude α) and Stokes field (amplitude β), both of which are far off resonance (see inset of Fig. 1). Accordingly the Raman laser is a special case of optically pumped three-level lasers for which lasing action is described by coupling the classical Maxwell field equation to the three-level density matrix equations and imposing a self-consistency requirement.[8,9] Defining δ_p (δ_s) as the normalized detuning of the pump (laser) emission from atomic resonance [$\delta_p=(\omega_p-\omega_{21})/\gamma$, $\delta_s=(\omega_s-\omega_{23})/\gamma$, where ω_p (ω_s) is the pump (laser) frequency and γ the material dephasing rate], then for Raman emission we take $\delta_p\sim\delta_s=\delta\gg 1$ and define $\Delta_s=\delta_s-\delta_p\ll\delta$. We further assume $|\alpha|^2/|\delta|^2\ll 1$, so ensuring that far off-resonant conditions persist in the presence of broadening arising from Rabi splitting of the pump transition. For these conditions we may set $\dot\rho_{21}=\dot\rho_{23}=0$, where ρ_{21} and ρ_{23} are the off-diagonal matrix elements for the pump and lasing transitions, respectively. This approximation is based on the "two-photon vector model" of Takatsuji[10] and Greschkovsky, Loymand, and Liano[11] as discussed in Ref. 7. Further, the population of the upper level ρ_{22}, which is approximately proportional to $|\alpha|^2/|\delta|^2$, is set to zero and we assume all the initial population resides in level 1. Under these conditions, and neglecting pump depletion, the six complex ordinary differential equations describing single-mode laser action in a three-level laser reduce to the following:

$$\dot\beta=-\sigma\beta-ig\frac{\alpha}{\delta}\rho_{31}^*-\frac{ig}{2\delta}\beta(1-D_{13})-i\theta\beta, \tag{1a}$$

$$\dot\rho_{31}=\{1+i[\Delta_s-\delta^{-1}(|\alpha|^2-|\beta|^2)]\}\rho_{31}-i(\alpha\beta^*/\delta)D_{13}, \tag{1b}$$

$$\dot D_{13}=-b(D_{13}-1)-\frac{2i}{\delta}(\alpha^*\beta\rho_{31}-\alpha\beta^*\rho_{31}^*), \tag{1c}$$

where $\theta=-\Delta_s+C$ is the cavity detuning; here $C=\omega_c-\omega_{23}-\delta$ and ω_c is the cavity frequency. The other physical parameters and variables are defined in Ref. 9. For comparison with the conventional Maxwell-Bloch equations we define $E=\beta$, $P=i\rho_{31}^*$, $W=-D_{13}$, and $A=\alpha$ which is a real constant to obtain

$$\begin{aligned}\dot E_s&=-\sigma E_s-(g/\delta)AP-(ig/2\delta)E_s(1+W)-i\theta E_s,\\ \dot P&=-(1-i\Delta)P+(A/\delta)E_sW,\\ \dot W&=-b(W+1)-(2A/\delta)(E_s^*P+E_sP^*),\end{aligned} \tag{2}$$

where $\Delta=\Delta_s-(A^2-|E_s|^2)/\delta$.

Inspection of these equations show their similarity with the Haken-Lorenz equations but with an additional third term on the right-hand side of the field equation. Also, Δ, which is the effective detuning from levels 1 to 3, modifies the detuning Δ_s through Stark shifts of the levels included by both the pump and lasing emission

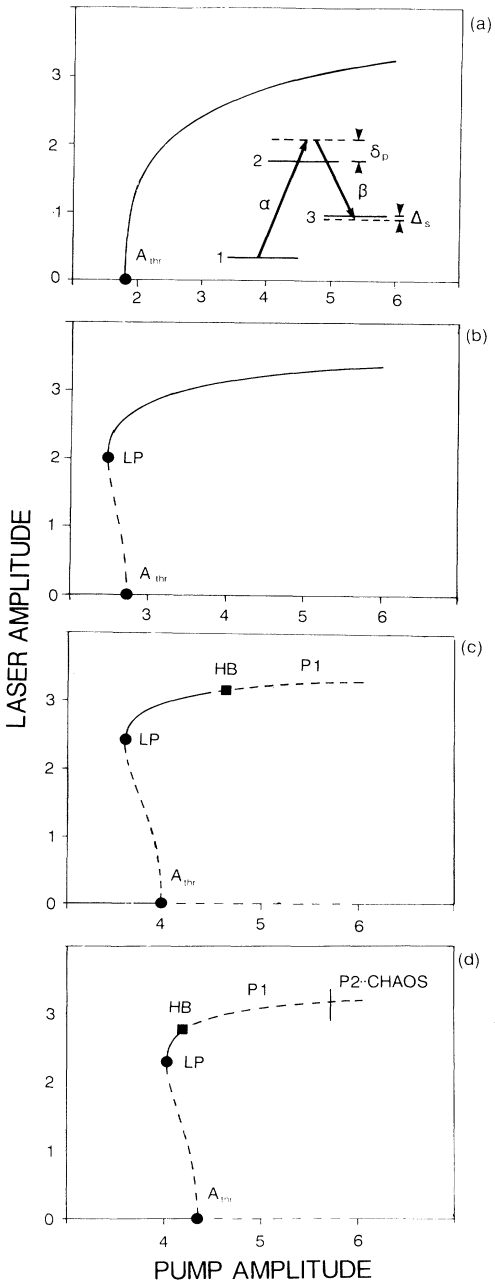

FIG. 1. Variation of the laser amplitude with pump amplitude as a function of detuning constant C. Solid lines denote branches of stationary solutions, dashed lines denote unstable stationary solutions. A_{thr}, LP, and HB represent laser threshold point, limit point, and Hopf bifurcation points, respectively. $C=0$, -4, -6.7, -7.4 correspond to (a)–(d). The other parameters are fixed at $g=180$, $\delta=14$, and $b=0.83$. Inset: Schematic of the Raman system considered in the analysis.

fields. Here levels 1 and 3 constitute the equivalent two-level system for which lasing occurs via a two-photon interaction of the pump and Stokes field generally in the absence of inversion. We also note that these equations reduce to those derived from the nonlinear-coupled-wave approach[6] on neglecting changes in population of the levels through omission of the population equation and the third term of the field equation. However, since this approximation is only valid when the pump field strength is insufficient to modify the level populations, it is unlikely to be justified for laser systems in which the internal cavity field strengths are in general high.

Our numerical analysis of Raman emission is based on Eq. (2) in which generally the dynamical behavior will depend on all of the control parameters. Here we consider the pump laser field amplitude A as our primary control parameter while the cavity loss σ, laser gain g, and the ratio b are held constant. We use as our secondary control parameter the cavity detuning C, the value of which we find has a critical bearing on whether laser emission is stable or unstable.

In general, the occurrences of dynamical instabilities have been found over a broad range of the control parameters; in parameter space (g,σ) occurring for $100<g<300$ and $0.5<\sigma<5$ dependent on the values of A and b, the parameter window for instabilities being larger for larger A and smaller b values over the respective range $3<A<6$ and $0.1<b<1$, δ is set at ~ 14. Full details of this parametrization will be reported elsewhere. By way of example, we consider here the case for $\sigma=3$, $b=0.83$, $\delta=14$, and $g=180$ for which bad cavity conditions prevail; $\sigma>1+b$. Figure 1 captures the laser emission characteristics under pump field variation for four equispaced values of the detuning constant C. The solid and dashed curves in each plot refer to branches of stable and unstable steady-state solutions. Branches of periodic and chaotic solutions in unstable regions are also identified in these plots. For $C=0$ [Fig. 1(a)] lasing is close to line center of the Raman gain and the first lasing threshold is correspondingly low. For cavity detuning values $C\geq 0$ emission exhibits similar characteristics; the threshold for lasing increasing and the emission field strength decreasing on increasing C. For detuning to the low-frequency side of gain line center, that is $C<0$, results are dramatically different. For example, for $C=-4$ [Fig. 1(b)] emission is bistable with the pump field strength giving stable nonlasing and lasing branches of solution as shown. Tracking along the nonlasing branch the solution remains stable with A until it reaches the point (A_{thr}) at which the branch loses stability. Beyond this point the unstable branch moves to lower A terminating at a limit point (LP) at which the upper branch of stable lasing solutions emanate for further increase of A. The value A_{thr} defines the first lasing threshold. These underlying bistable features persist for further negative detuning; the first lasing threshold steadily increasing in A with increase in cavity detuning. As discussed below, it is in this region that we identify periodic and aperiodic pulsating instabilities in the Raman emission which originate from both stable steady-

state lasing and at the onset of lasing.

The origin of this dynamical behavior and bistability lies in the emission-field-induced asymmetric distortion of the dispersion profile and its relative displacement from the associated gain profile. We emphasize that, as a consequence of off-resonant pumping, the homogeneously broadened Raman gain profile remains symmetric and single peaked for all levels of pumping; the influence of the pump is only in determining the magnitude of the Raman gain and in small frequency shifting of the gain profile as described through the detuning factor Δ discussed above. Full details of this analysis will be published elsewhere. In contrast for resonantly coupled three-level systems, the gain profile is modified by pump-induced Rabi splitting resulting in a symmetric double-peaked gain distribution about the laser transition for typical pump field strengths.[12] This plays a central role in determining the dynamical behavior of this system[9,13-21] and in distinguishing it from two-level systems.[9,13,15,20,21] In this respect Raman systems are more readily identified with the Haken-Lorenz model as established mathematically through Eq. (2).

Partial results of dynamical behavior are shown in Figs. 1(c) and (d) for cavity detunings of $C=-6.7$ and -7.4, respectively. For $C=-6.7$ the upper branch of solutions show steady-state lasing, the field amplitude steadily increasing with increasing pump field to a value of 4.5 at which the solution loses stability through a Hopf bifurcation. This gives rise to a branch of periodic solutions, nonsymmetric about the nonlasing branch, whose amplitude and frequency increase by less than 10% over a unit increase of pump amplitude from a value in the proximity of the Hopf bifurcation. These effects are attributed to the pump-field-induced frequency shift of the Raman gain profile across the fixed cavity frequency. For increased cavity detuning $C=-7.4$ [Fig. 1(d)] it is seen that while the first lasing threshold (A_{thr}) continues to increase in A the Hopf bifurcation point moves to lower A with a consequent reduction in the range of pumping over which stable lasing occurs. Notably, for this case the onset of lasing via bistability is to an unstable branch of solutions. On increasing A, emission evolves into chaos through a period-doubling bifurcation sequence. Representative phase portraits of the basic oscillation, $2P$ bifurcation and chaotic emission, are shown in Fig. 2 plotted in a $(|E_s|,W)$ parameter space. Here negative and positive values of W are for noninverted and inverted population differences between levels 3 and 1. The trajectories show the dynamics of the system to be predominantly in a noninverted state, inversion occurring when the pulsating emission field strength is high. The trajectories for the $1P$ limit cycle increase with pump field amplitude to a value which remains essentially constant for subsequent bifurcations to chaos. Here excursions of the emission field amplitudes are sufficiently large to take them close to the unstable manifold of the nonlasing branch. This is reflected in the distortion of the $2P$ limit cycle and chaotic attractor.

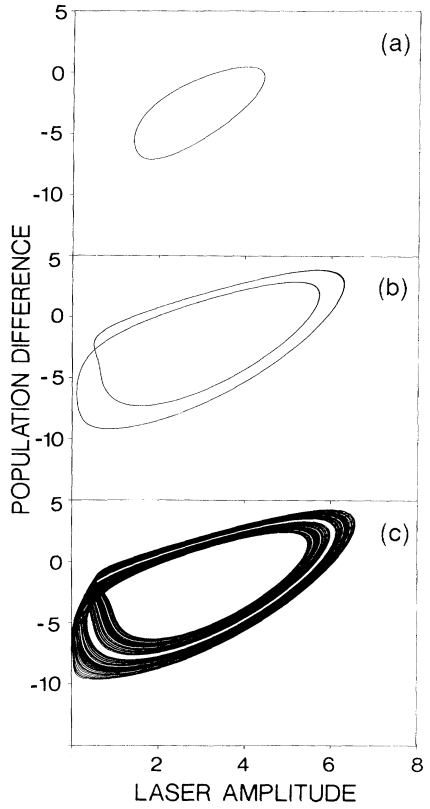

FIG. 2. A two-dimensional phase portrait $(|E_s|,W)$ for pump amplitudes. Other parameters are fixed. $g=180$, $\delta=14$, $b=0.83$. (a) $A=4.60$, (b) 5.70, (c) 5.88.

In Fig. 3 we show the variation of the Raman emission field amplitude with cavity tuning for two representative values of pump field amplitude, $A=2.5$ and 5.4 (compare with Fig. 1). As expected the tuning range is larger for the higher pump level due to the increased Raman gain. The asymmetry in the emission field amplitude in both curves is a manifestation of the laser-field-induced distortion of the dispersion profile as discussed earlier. We note that for weak lasing emission the gain and dispersion profiles tend to be symmetric and the maximum lasing emission is obtained at $C=A^2/\delta$ close to zero. For increasing field emission, the field-induced asymmetry in the dispersion profile results in a shift in the peak of the laser emission to negative detuning from $C=0$. It is in this region that dynamical instabilities and bistability occur depending on the field amplitude. While stable emission is obtained for the low pump level (curve 1), for the higher value (curve 2) instabilities occur as expected over a range of cavity tuning (dashed curve) to the low-frequency side of the zero value. Significantly, this region extends to that for which the emission field is a maximum. Accordingly dynamical instabilities are favored for conditions in which Raman lasing is optimum.

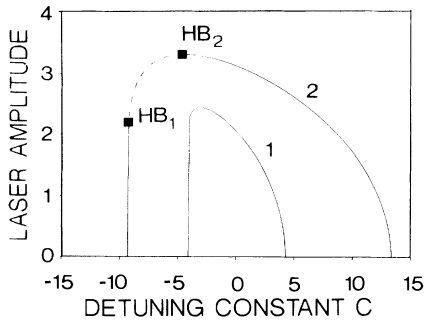

FIG. 3. Asymmetry of laser field amplitude with detuning constant C for $A=2.5$ (curve 1) and $A=5.4$ (curve 2). Other parameters are as in Fig. 2. Solid and dashed lines denote branch of stationary and unstable solutions, respectively. Closed squares represent two Hopf bifurcation points (HB_1 and HB_2).

Finally, we compare the above results with earlier observations of the dynamical instabilities of the 12.8-μm emission from NH_3 optically pumped on the $aR(6,0)$ transition 1.3 GHz below the line center 1; the parameter values of which fall well within those discussed earlier. The onset of instabilities via a period-doubling route to chaos [$P1\sim 18$ nsec (experiment), 14 nsec (theory)] accompanied by bistable switching (compare emission and pump profiles of Ref. 1) occurs for a pump intensity close to the lasing threshold [~ 40 kW/cm^2 internal to cavity (experiment), ~ 54 kW/cm^2 for $A_{th}\sim 4$ (theory)] for an asymmetric cavity detuning range from gain center [~ 0.2 of the full lasing range (experiment and theory)] close to that for maximum lasing.

In conclusion, nonlinear dynamical and bistable behavior in the emission from a single-mode homogeneously broadened Raman laser has been identified, the features and operating conditions of which are in good agreement with earlier experiments. As systems reducible to a simple mathematical description, similar to that of the Haken-Lorenz model but for which operating conditions are considerably relaxed, they provide excellent opportunity for quantitative tests of nonlinear dynamics, operation being within easy access of experiments for this broad class of laser system.

This work was supported by the Science and Engineering Research Council (United Kingdom). W.L. is supported by The Royal Society of London. We wish to thank J. V. Moloney, L. A. Lugiato, and L. M. Narducci for helpful discussions.

[a]On leave from Shanghai Institute of Optics and Fine Mechanics, Shanghai, People's Republic of China.

[1]R. G. Harrison and D. J. Biswas, Phys. Rev. Lett. **55**, 63 (1985); D. J. Biswas and R. G. Harrison, Opt. Commun. **54**, 112 (1985); Appl. Phys. Lett. **47**, 198 (1985).

[2]R. G. Harrison, W. Lu, and P. K. Gupta, in Proceedings of Noise and Chaos in Nonlinear Dynamical Systems, Turin, Italy, 7–11 March 1989 (NATO Advanced Research Workshop, to be published).

[3]H. Haken, Phys. Lett. **53A**, 77 (1975).

[4]L. M. Narducci, M. Sadiky, L. A. Lugiato, and N. B. Abraham, Opt. Commun. **55**, 370 (1985).

[5]H. Zeghlache and P. Mandel, J. Opt. Soc. Am. B **2**, 18 (1985).

[6]Y. R. Shen, *The Principles of Nonlinear Optics* (Wiley, New York, 1984).

[7]M. G. Raymer, J. Mostowski, and J. L. Carlsten, Phys. Rev. A **19**, 2304 (1979).

[8]M. A. Dupertuis, R. R. E. Salomma, and M. R. Siegrist, Opt. Commun. **57**, 40 (1986).

[9]J. V. Moloney, J. S. Uppal, and R. G. Harrison, Phys. Rev. Lett. **59**, 2868 (1987).

[10]M. Takatsuji, Phys. Rev. A **11**, 619 (1975).

[11]D. Grischkowsky, M. M. Loymand, and P. F. Liano, Phys. Rev. A **12**, 2514 (1975).

[12]R. L. Panock and R. J. Temkin, IEEE J. Quantum Electron. **13**, 425 (1977).

[13]S. C. Mehendale and R. G. Harrison, Phys. Rev. A **34**, 1613 (1986); Opt. Commun. **60**, 257 (1986).

[14]T. C. Ryan and N. M. Lawandy, IEEE J. Quantum Electron. **22**, 2075 (1986).

[15]J. S. Uppal, R. G. Harrison, and J. V. Moloney, Phys. Rev. A **36**, 4823 (1987).

[16]J. Pujol, R. Vilaseca, R. Corbolan, and F. Aguarta, Int. J. Infrared Millimeter Waves **8**, 299 (1987).

[17]J. C. Ryan and N. M. Lawandy, Opt. Commun. **64**, 54 (1987).

[18]P. A. Khandokhin, Ya. I. Khanin, and I. V. Koryukin, Opt. Commun. **65**, 367 (1988).

[19]J. Pujol, F. Laguarta, R. Vilaseca, and R. Corbolan, J. Opt. Soc. Am. B **5**, 1004 (1988).

[20]J.V. Moloney, W. Forysiak, J. S. Uppal, and R. G. Harrison, Phys. Rev. A **39**, 1277 (1989).

[21]W. Forysiak, R. G. Harrison, and J. V. Moloney, Phys. Rev. A **39**, 421 (1989).